*J Physiol* 587.11 (2009) pp 2443–2455



The Journal of Physiology

# Switching between transient and sustained signalling at the rod bipolar-AII amacrine cell synapse of the mouse retina

Josefin Snellman[2], David Zenisek[2] and Scott Nawy[1]

[1]*Department of Ophthalmology and Visual Sciences, Dominick P. Purpura Department of Neuroscience, Albert Einstein College of Medicine, The Rose F. Kennedy Center, 1410 Pelham Parkway South, Bronx, NY 10461, USA*
[2]*Yale University School of Medicine, Department of Cellular and Molecular Physiology, Yale University School of Medicine, 333 Cedar Street, SHM-B103, New Haven, CT 06520, USA*

**At conventional synapses, invasion of an action potential into the presynaptic terminal produces a rapid $Ca^{2+}$ influx and ultimately the release of synaptic vesicles. However, retinal rod bipolar cells (RBCs) generally do not produce action potentials, and the rate of depolarization of the axon terminal is instead governed by the rate of rise of the light response, which can be quite slow. Using paired whole-cell recordings, we measured the behaviour of the RBC-AII amacrine cell synapse while simulating light-induced depolarizations either by slowly ramping the RBC voltage or by depolarizing the RBC with the mGluR6 receptor antagonist (*R*,*S*)-α-cyclopropyl-4-phosphonophenylglycine (CPPG). Both voltage ramps and CPPG evoked slow activation of presynaptic $Ca^{2+}$ currents and severely attenuated the early, transient component of the AII EPSC compared with voltage steps. We also found that the duration of the transient component was limited in time, and this limitation could not be explained by vesicle depletion, inhibitory feedback, or proton inhibition. Limiting the duration of the fast transient insures the availability of readily releasable vesicles to support a second, sustained component of release. The mGluR6 pathway modulator cGMP sped the rate of RBC depolarization in response to puffs of CPPG and consequently potentiated the transient component of the EPSC at the expense of the sustained component. We conclude that the rod bipolar cell is capable of both transient and sustained signalling, and modulation of the mGluR6 pathway by cGMP allows the RBC to switch between these two time courses of transmitter release.**

(Received 10 November 2008; accepted after revision 26 March 2009; first published online 30 March 2009)
**Corresponding author** S. Nawy: Department of Ophthalmology and Visual Sciences, Dominick P. Purpura Department of Neuroscience, Albert Einstein College of Medicine, The Rose F. Kennedy Center, 1410 Pelham Parkway South, Bronx, NY 10461, USA. Email: nawy@aecom.yu.edu

**Abbreviations** L-AP4, L(+)-2-amino-4-phosphonobutyric acid; CPPG, (*R*,*S*)-α-cyclopropyl-4-phosphonophenylglycine; QX-314, *N*-(2,6-dimethylphenylcarbamoylmethyl)triethylammonium bromide; 8-pCPT-cGMP, 8-(4-parachlorophenylthio)-cGMP; PTX, picrotoxin; RBC, rod bipolar cell; RRP, readily releasable pool; TBOA, DL-threo-β-benzyloxyaspartate; TPMPA, 1,2,5,6-tetrahydropyridin-4yl-methylphosphinic acid.

Rod bipolar cells (RBCs) are a specialized class of On bipolar cell that collect input from rods and synapse onto the AII amacrine cell, creating a scotopic-specific circuit in the mammalian retina (Bloomfield, 2001). In studies where voltage steps were used to stimulate synaptic transmission, release of vesicles from RBC presynaptic terminals was found to be highly synchronized, producing a large transient component of the EPSC in the AII amacrine cell. A small sustained component of the EPSC was also observed, and was attributed to ongoing replenishment of the depleted pool of readily releasable vesicles (RRP) (Singer & Diamond, 2003; Singer *et al.* 2004; Singer & Diamond, 2006). On the other hand, studies of the AII EPSC using light as a stimulus have reported a more even mixture of transient and sustained components (Nelson, 1982; Xin & Bloomfield, 1999; Bloomfield & Xin, 2000; Volgyi *et al.* 2002; Wu *et al.* 2004; Trexler *et al.* 2005; Dunn *et al.* 2006; Pang *et al.* 2007). The discrepancy between these two approaches may be due to differences in the parameters of the stimuli: the amplitude of RBC responses to saturating light intensities generally does not exceed about 20 mV (Berntson & Taylor, 2000; Trexler *et al.* 2005), much smaller than the voltage excursions used in voltage step studies. In fact, responses to the absorption of single photons can be detected in the inner retina (Robson &


DOI: 10.1113/jphysiol.2008.165241

Frishman, 1995; Saszik *et al.* 2002), indicating that the RBC–AII synapse can operate under conditions where the presynaptic voltage change is considerably less than 20 mV. Furthermore, voltage steps do not closely mimic the rate of light-induced RBC depolarization. Although some On type bipolar cells do exhibit fast, regenerative responses to light (Protti *et al.* 2000; Ichinose *et al.* 2005), light-evoked depolarizations are generally quite slow, with a time to peak of 100–130 ms (Euler & Masland, 2000; Berntson *et al.* 2004; Trexler *et al.* 2005).

One goal of the present study was to reconcile these two observations by characterizing the AII amacrine cell EPSC as a function of the rate of RBC membrane depolarization. To accomplish this, we injected voltage steps and ramps into RBCs and measured the response of synaptically connected AIIs. We find that the shape of the EPSC is strongly dependent on the rate of RBC depolarization, with faster depolarizations producing EPSCs with a dominant transient component, and slower rates resulting in mainly sustained release.

In addition to ramps, we wanted to use a more physiological stimulus to depolarize the RBC. Normally, light depolarizes RBCs by turning off synaptic glutamate release. Glutamate binds to the mGluR6 receptor, which is expressed in the dendrites of RBCs (Nakajima *et al.* 1993; Vardi *et al.* 1998), and couples negatively to a cation-selective transduction channel (Shiells *et al.* 1981; Slaughter & Miller, 1981). By suppressing the release of glutamate, light indirectly shuts off the mGluR6 cascade, leading to activation of the transduction channel and depolarization of the RBC. The action of light can be mimicked pharmacologically by local application of an mGluR6 antagonist (Snellman & Nawy, 2002; Nawy, 2004). Here, using simultaneous current clamp of a RBC and voltage clamp of a synaptically connected AII amacrine cell, we show that local application of the mGluR6 antagonist resulted in relatively slow RBC depolarizations resulting in primarily sustained EPSCs. However, the mGluR6 cascade modulatory agent cGMP (Snellman & Nawy, 2004) significantly sped up depolarization. The increase in the rate of depolarization led to a significant enhancement of the transient component of the EPSC. Our results imply that transient and sustained signals do not have to be conveyed by separate cell types, as a single class of On bipolar cell can transmit both types of signals, and that cGMP may provide a physiological switch from sustained to transient synaptic transmission.

## Methods

### Slice preparation and solutions

Retinal slices from 4- to 6-week-old C57/BL6 mice (Charles River) were prepared as described previously (Snellman & Nawy, 2004). All procedures were approved by the Institute for Animals Studies at the Albert Einstein College of Medicine. Mice were anaesthetized with halothane (Sigma), killed by cervical dislocation, and their eyes removed and enucleated. Whole retinas were isolated and placed on a 0.65 $\mu$m cellulose acetate/nitrate membrane filter (Millipore), which was secured with vacuum grease to a glass slide adjacent to the recording chamber. Slices were then cut to a thickness of 150 $\mu$m using a tissue slicer (Stoelting Co. Wood Dale, IL, USA), transferred to the recording chamber while remaining submerged, and viewed with a Zeiss Axioskop equipped with a water-immersion 40× DIC objective. The recording chamber was immediately attached to a perfusion system and the slices were perfused at a rate of 5 ml min$^{-1}$ with Ames medium bubbled with 95% $O_2$–5% $CO_2$. The bath solution was supplemented with 100 $\mu$M picrotoxin and 50 $\mu$M 1,2,5,6-tetrahydropyridin-4yl-methylphosphinic acid (TPMPA) to block $GABA_A$ and $GABA_C$ receptors, and 10 $\mu$M strychnine to block glycine receptors. During experiments using (*R*,*S*)-$\alpha$-cyclopropyl-4-phosphonophenylglycine (CPPG) stimulation, 5 $\mu$M L(+)-2-amino-4-phosphonobutyric acid (L-AP4) was included in the bath. CPPG (600 $\mu$M) was delivered to the dendrites of the rod bipolar cells by applying positive pressure (2–3 p.s.i.) to a fine pipette using a Picospritzer III (Parker-Hannifin, Cleveland, OH, USA). For experiments using 20 mM Hepes, the bath solution was composed of (in mM): 112.5 NaCl, 20 $NaHCO_3$, 2.6 KCl, 1.2 $CaCl_2$, 2.4 MgCl, 10 glucose, 20 Hepes, 3 sodium succinate. The standard recording solution for rod bipolar cells was composed of (in mM) 125 potassium gluconate, 2 EGTA, 10 KCl, 10 Hepes, 4 MgATP, 1 LiGTP. For isolation of calcium currents in rod bipolar cells, the recording solution contained (in mM): 108 gluconic acid, 2 EGTA, 10 CsCl, 10 TEA, 4 MgATP, 1 LiGTP. The amacrine cell internal solution was composed of (in mM): 125 potassium gluconate, 10 EGTA, 10 Hepes, 10 KCl, 4 MgATP, or 100 $CsCH_3SO_3$, 10 EGTA, 20 TEA, 10 Hepes, 4 MgATP. *N*-(2,6-Dimethylphenylcarbamoylmethyl)triethylammonium bromide (QX-314) at 2 mM was added to block action potentials. The pH was adjusted to 7.4 with NaOH for sodium based solutions, KOH for potassium based solutions, and CsOH for caesium based solutions. Alexa Fluor 488 or 594 (14 $\mu$g ml$^{-1}$) was added to all the recording solutions to visualize cells. The osmolarity of both extracellular and intracellular solutions was 289–293 mosmol l$^{-1}$, with a pH of 7.35–7.40.

All chemicals were obtained from Sigma, except for CPPG, L-AP4, TPMPA, DL-threo-$\beta$-benzyloxyaspartate (TBOA) and cyclothiazide (Tocris), Alexa Fluor (Molecular Probes/Invitrogen), and 8-(4-parachlorophenylthio)-cGMP (8-pCPT-cGMP; Calbiochem). 8-pCPT-cGMP was stored as powder at −20°C and added to solutions immediately before use. CPPG and L-AP4

were stored as stock solutions at 4°C and added to bath and puffer solutions immediately before use. All other drugs were aliquoted, stored at −20°C, and dissolved in pipette solution on the day of use.

### Electrophysiology and analysis

Patch pipettes of resistance 8–11 MΩ were fabricated from borosilicate glass (WPI) using a two-stage vertical puller (Narishige). Pipettes used for recording of calcium currents were coated with sylgard (Dow Corning Corp.) or Sticky wax (Kerr Corp. Orange, CA, USA). Whole-cell recordings were obtained using an Axopatch 200A and Axopatch 1D amplifiers (MDC), or a dual EPC10 amplifier (HEKA Instruments Inc., Bellmore, NY, USA). The input/series resistances of the RBC and AII amacrine cell recordings were approximately 3 GΩ/15–20 MΩ, and 1 GΩ/20–25 MΩ, respectively. Cells were discarded if the series resistance exceeded 40 MΩ, or if the holding current changed suddenly. Holding potentials were corrected for the liquid junction potential, which was measured to be −12 mV, or −15 mV depending on solutions. Rod bipolar and AII amacrine cells were identified by their shape and position in the slice, as determined by fluorescence imaging. Images were captured and stored with a CCD camera (COHU Electronics) and frame grabber (Scion Corp. Frederick, MA, USA). Data were acquired with either Axograph and the Digidata 1200 interface (MDC) or PatchMaster (HEKA Instruments).

Analysis was performed using Axograph X, Kaleidagraph (Synergy Software, Reading, PA, USA) or Igor Pro (WaveMetrics, Inc., Lake Oswego, OR, USA). Currents were elicited at 20–40 s intervals, collected at 20 kHz, and in some cases low-pass filtered at 1 kHz. Rod bipolar cell calcium currents were leak subtracted using a *P*/4 protocol. We measured the rate of RBC depolarization either by dividing the amplitude of the response by the 10–90% rise time, or fitting a line by eye to the first 50% of the rising phase of the response. Both methods produced similar results and only the 10–90% method is reported here. Results are represented as the mean ± S.E.M. Statistical significance was determined using Student's paired or unpaired *t* test, with * indicating $P < 0.02$ and ** indicating $P < 0.01$.

## Results

### The transient nature of the AII EPSC is not due to depletion of the readily releasable vesicle pool

Rod bipolar cells (RBCs) and AII amacrine cells were identified in slices of mouse retina by their characteristic shapes (Fig. 1*A*, left). Under voltage clamp, steps to membrane potentials more positive than −45 mV in the RBC typically elicited an EPSC in the AII amacrine cell (Fig. 1*A*, middle). Near threshold, the timing of the EPSC was not well synchronized to the onset of the voltage step, and both its amplitude and time course were similar to the averaged spontaneous EPSC (inset). The EPSC amplitude rose steeply with RBC voltage, reaching a half-maximal response at −38 mV, and saturating near −31 mV (Fig. 1*A*, right). Voltage steps that elicited at least a half-maximal response evoked a sustained $Ca^{2+}$ current in RBCs and a highly synchronized, transient EPSC (10–90% value: 1.2 ± 0.08 ms, $n = 10$) in the AII amacrine cell (Fig. 1*B*). The EPSC reflects the time course of release of the RRP at the RBC terminal (Mennerick & Matthews, 1996; von Gersdorff *et al.* 1998; Singer & Diamond, 2003).

The observation that the transient AII EPSC decays to baseline in the presence of a sustained presynaptic $Ca^{2+}$ influx has been interpreted to reflect depletion of the RRP (Singer & Diamond, 2006). If the decay were due to the depletion of docked vesicles from the ribbon, then smaller depolarizations which produced submaximal responses in the AII would be expected to prolong the duration of this component of release. We found that this was not the case (but see Singer & Diamond, 2003). Figure 1*C* illustrates the results of an experiment where EPSCs were generated by three voltage steps of increasing amplitude. A 60 ms voltage step to −31 mV produced an EPSC of maximum amplitude, as increasing the step amplitude to −19 mV had no further effect, while a step to −37 mV produced an EPSC which was approximately 50% of maximum. The duration of the transient component of the EPSC, measured as the width of the response at 50% of the peak, was nearly identical for both maximal and half-maximal responses (Fig. 1*C*, inset). The mean width of the half-maximal response was 4.5 ± 0.7 ms, compared with 4.8 ± 0.5 ms for the maximum response ($n = 11$, $P > 0.6$). Further evidence against depletion of the RRP was obtained by calculating the quantal content of the transient component of the EPSC. For each RBC–AII pair, we estimated the quantal content by dividing the charge of the transient component by the total charge of the averaged elementary event. We obtained an average of 26 vesicles per voltage step (26.1 ± 2.0, $n = 11$), well below the estimated RRP size of 70 vesicles in rat RBCs (Singer & Diamond, 2006). Thus, even for depolarizing stimuli that are too weak to deplete all of the vesicles from the readily releasable pool, the duration of the initial rapid phase of transmitter release is limited (Hsu *et al.* 1996; Burrone & Lagnado, 2000; Wolfel *et al.* 2007), indicating that there is an intrinsic mechanism that prevents extended periods of coordinated release of multiple vesicles from the ribbon.

A number of different mechanisms have been shown to impose limits on transmitter release. One possibility is that inhibitory feedback from amacrine cells (Hartveit, 1999; Singer & Diamond, 2003; Chavez *et al.* 2006; Eggers & Lukasiewicz, 2006; Chavez & Diamond, 2008) limits the duration of the transient component of the EPSC.

To test this, we applied voltage steps of 10, 20 and 30 ms in the presence of picrotoxin (PTX), TPMPA and strychnine. With inhibition blocked, the duration of the fast component was the same regardless of the length of the stimulus (Fig. 1*D*, left). The primary effect of longer steps was to augment the sustained component of the EPSC. Thus, inhibitory feedback seems unlikely to play a significant role in shaping the transient component. Proton inhibition of $Ca^{2+}$ current in RBC terminals can also decrease release (Palmer *et al.* 2003). However, buffering of protons with 20 mM Hepes and 20 mM bicarbonate in the bath solution did not significantly change the half-width of the transient component in response to a series of voltage steps (Fig. 1*D*, middle). As a further test, we compared the mean half-width of the transient component in high Hepes solution with the value obtained in control solution. The half-width measured in Hepes was $5.3 \pm 0.4$ ms, ($n = 6$), while the value in control solution (as reported above for a 20 mV step) was $4.8 \pm 0.5$ ms ($n = 11$). The difference was not significant ($P > 0.40$, Student's unpaired $t$ test), further evidence that proton inhibition does not limit the duration of the transient component.

Synaptic transmission can also be inhibited by activation of a presynaptic glutamate transporter which couples to a membrane-hyperpolarizing anion current

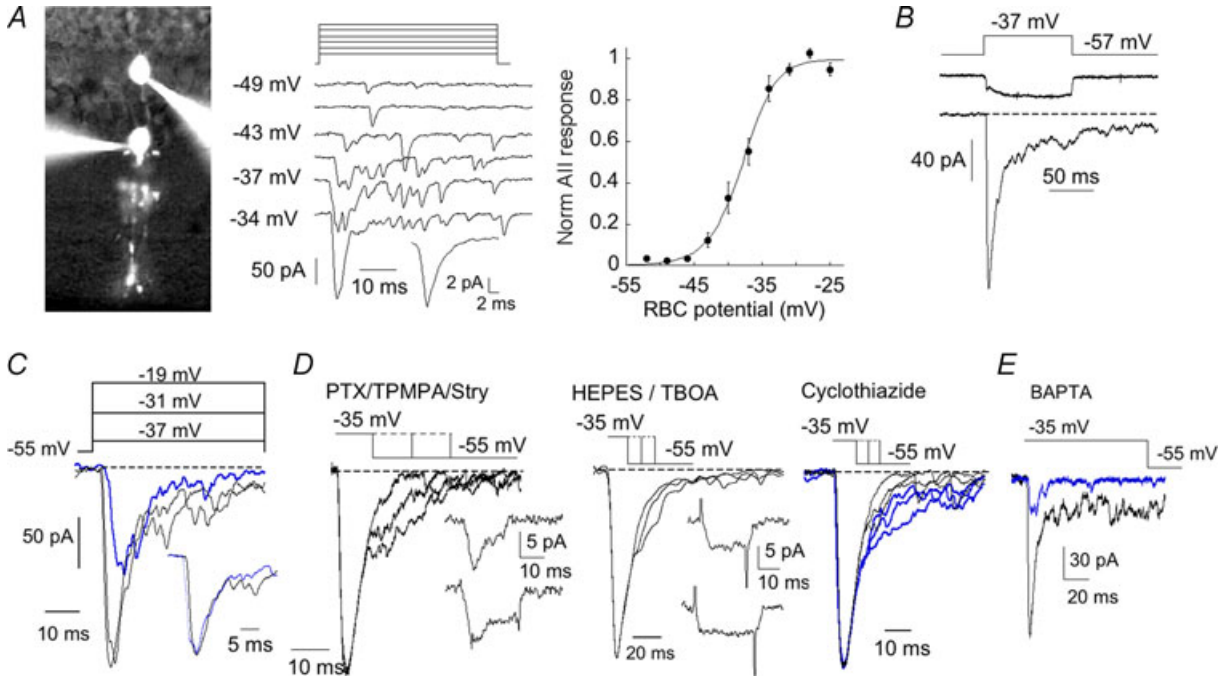


**Figure 1. Paired recordings from rod bipolar and AII amacrine cells reveal a transient and sustained component of the postsynaptic response to voltage steps**

*A*, left, image of a RBC and AII amacrine cell pair visualized by injection of Alexa 488 through the recording pipettes. Middle, family of AII amacrine EPSCs evoked by a series of voltage steps in a presynaptic RBC. Duration of the steps was 50 ms. Series was from −49 mV to −34 mV in 3 mV increments. Inset, averaged spontaneous EPSC obtained from the same cell. Right, summary of the AII response as a function of presynaptic voltage ($n = 9$ cells). *B*, depolarizing 100 ms step in a RBC elicited a sustained $Ca^{2+}$ current in the RBC and a transient EPSC in the AII amacrine. *C*, comparison of the kinetics of the response to a voltage step that was half-maximal (in this pair, a step to −37 mV) and maximal (−31 mV). Response to a step to −19 mV is also shown. Each trace is the average of 3–5 responses. Inset, Normalization of the half-maximal and maximal responses reveals a similarity of the kinetics of the fast component. *D*, left, AII responses from one cell to 10, 20 and 30 ms voltage steps of 20 mV in the presence of 100 $\mu$M PTX, 50 $\mu$M TPMPA and 10 $\mu$M strychnine. Inset, corresponding RBC calcium currents recorded during the 20 ms (top) and 30 ms steps. Middle, responses to 15, 25 and 35 ms (20 mV) voltage steps in the presence of bath applied Hepes (20 mM), bicarbonate (20 mM) and TBOA (75 $\mu$M). Inset, corresponding RBC calcium currents from the 20 ms (top) and 30 ms steps. Note that the superimposed outward current, which can be observed in the control traces to the left, is blocked by Hepes and TBOA. Right, responses from an AII cell to 20 mV steps of 10, 15 and 20 ms duration in the absence (black, thin line) and presence (blue in the online version, thick line) of cyclothiazide. The peaks of the responses have been scaled in all three panels. *E*, single raw traces showing the response in an AII cell to a 20 mV step in an RBC immediately after break in (black, thin line) and after 5 min of recording (blue in the online version, thick line) with an internal solution containing 6 mM BAPTA. Normal internal solution was used for the AII recording (see Methods).

(Veruki *et al.* 2006; Wersinger *et al.* 2006). However, following addition of the excitatory amino acid transporter (EAAT) inhibitor TBOA (75 $\mu$M) to the bath, the half-width remained insensitive to changes in the duration of the voltage step (Fig. 1*D*), and the mean half-width of the response in TBOA was not significantly different from control (half-width $5.5 \pm 0.3$, $n = 4$, $P > 0.24$ compared with control). Although it had no discernable effect on the duration of the EPSC transient, TBOA eliminated the time-dependent reduction in the recorded calcium currents (compare insets Fig. 1*D*, left and middle). This effect of TBOA has been observed previously (Veruki *et al.* 2006) and attributed to the superimposed activation of the glutamate transporter current.

The decay of the transient component is unlikely to result from postsynaptic AMPA receptor desensitization since the decay of the response is substantially faster than the reported rate of desensitization of the postsynaptic AMPA receptors (Veruki *et al.* 2003) and because this component of the EPSC persists in the presence of cyclothiazide (Singer & Diamond, 2003). Furthermore, addition of 50 $\mu$M cyclothiazide to the bath increased the peak of the transient component of the EPSCs, but did not change its kinetics compared to control (Fig. 1*D*, right, $n = 4$; $P > 0.22$ compared with control).

We considered the possibility that the width of the transient component of the EPSC might be limited by the kinetics of $Ca^{2+}$ buffering by EGTA. To test this possibility, we buffered rod bipolar cells with the fast $Ca^{2+}$ chelator BAPTA, instead of EGTA. Immediately after break-in, the amplitude of the fast component was similar to responses observed in EGTA-buffered rod bipolar cells (Fig. 1*E*, $102.7 \pm 26.0$ pA, $n = 5$). However, after 5 min of dialysis with 2–6 mM BAPTA, the peak decreased significantly ($18.9 \pm 2.6$ pA, $P = 0.02$, Student's paired $t$ test). These results are consistent with the idea that faster buffering of $Ca^{2+}$ attenuates the peak of the EPSC because it reduces the delay between $Ca^{2+}$ influx and buffering.

### Slow depolarizations of the rod bipolar cell elicit sustained responses in the postsynaptic AII amacrine cell

The terminals of RBCs do not typically depolarize as rapidly as the presynaptic terminals of neurons which are invaded by action potentials. Instead, they depolarize to light in a graded manner with the speed of depolarization being a function of light intensity. To determine how the shape of the AII EPSC would be altered by more gradual depolarizations, we ramped the membrane potential of RBCs from −57 mV to −37 mV at rates that varied from 2000 mV $s^{-1}$ to less than 100 mV $s^{-1}$. Ramping the RBC membrane potential at a rate of 2000 mV $s^{-1}$ (i.e. ramp length of 10 ms) most closely approximated the postsynaptic response elicited by a step (Fig. 2*A*), evoking a fast rising EPSC which decayed exponentially. With decreasing ramp speeds, the transient component of the EPSC became smaller and more sustained, lacking the early transient component of the EPSC that reflects fast release of transmitter. The peak amplitude of the EPSC declined exponentially with decreasing rates of RBC depolarization, until it reached approximately 50% of the response obtained with an instantaneous step of the same magnitude (Fig. 2*B*, left). The total charge transfer elicited by ramps increased with ramp duration, reaching a steady state at ramp durations of about 50 ms (Fig. 2*B*, right). The steady state is likely to reflect depletion of the RPP since the maximum number of released vesicles during a ramp stimulus was calculated to be $72.5 \pm 11.8$, similar to the size of the RRP at this synapse reported previously (Singer & Diamond, 2006). Our findings are consistent with the idea that slowing the rate of RBC depolarization favours sustained, uncorrelated release which continues until the RRP is depleted.

Once the sustained, uncorrelated mode of release was activated, we found that it was difficult to switch to the transient, synchronous mode. This is illustrated in Fig. 2*C*, which shows the response of an AII to $Ca^{2+}$ tail currents under two different conditions. On the left, a 5 ms ramp from −57 mV to −37 mV is too brief to evoke an EPSC, but following repolarization to −57 mV, the resulting tail current consistently evoked a fast EPSC. The tail current evoked the release of approximately five quanta during the first 2 ms ($5.3 \pm 0.8$ quanta, $n = 6$ pairs). In contrast, a 20 ms ramp elicited an EPSC, but a $Ca^{2+}$ tail current at the end of the ramp evoked a very small response, containing less than a single quantum per stimulus in the first 2 ms ($0.6 \pm 0.3$ quanta, $n = 6$ pairs). This could result from depletion of the RRP by the ramp stimulus. However, analysis of total charge transfer as a function of ramp length suggests that a 20 ms ramp does not result in full depletion of the RRP: On average, a 20 ms ramp evoked only about 60% of the RRP ($n = 6$, Fig. 2*B*, right panel), implying the presence of additional docked vesicles that are not released by the $Ca^{2+}$ tail current at the end of the 20 ms ramp. This estimate assumes that refilling of the RRP is minimal during ramp stimulation, as 100 ms is not thought to be sufficient for significant reloading of vesicles onto the ribbon (Mennerick & Matthews, 1996).

Loss of the transient phase of the EPSC during slow ramps did not result from a reduced presynaptic $Ca^{2+}$ current since $Ca^{2+}$ currents elicited by slow ramps ultimately reached the same amplitude and carried larger charge than currents elicited by faster ramps. Furthermore, the peak of the $Ca^{2+}$ current was delayed compared to the peak of the AII EPSC (see Fig. 3*A*, as well as Nelson, 1982), making it unlikely that the amplitude of the $Ca^{2+}$ current determined whether the synapse output was transient or sustained. In support of this idea, voltage ramps to the

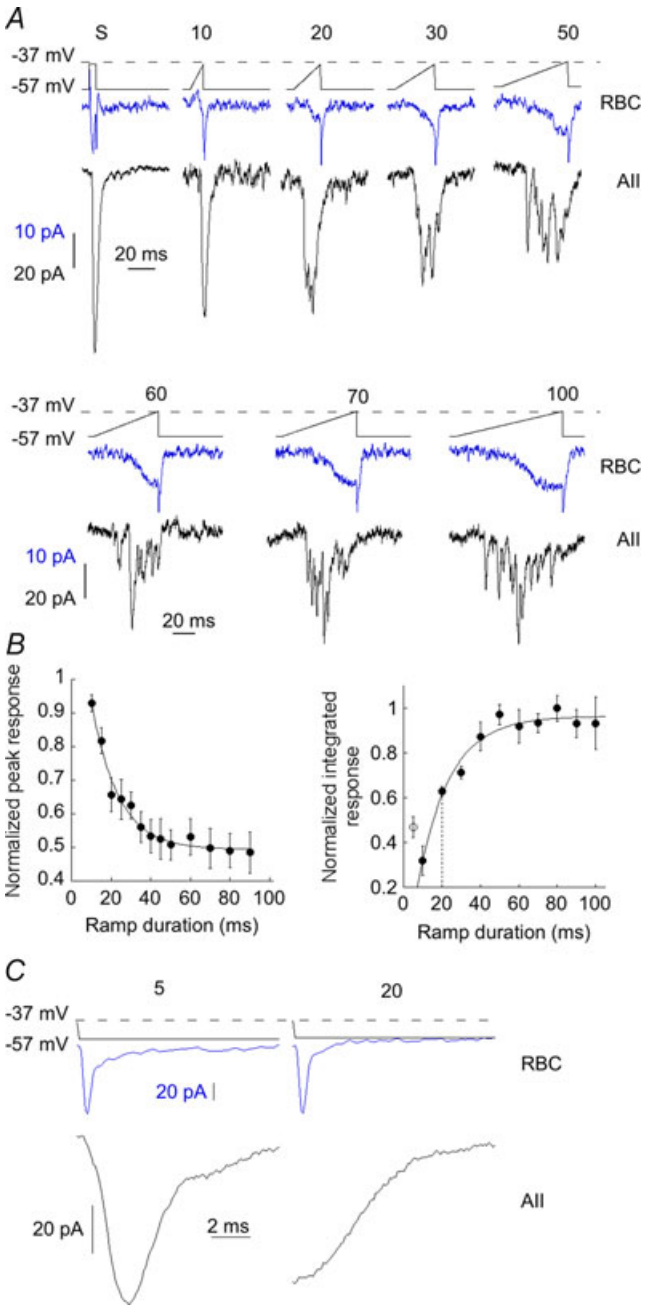


**Figure 2. Rapid depolarization of the RBC enhances the transient component of the EPSC**
*A*, responses from an RBC–AII pair. Upper traces are the RBC $Ca^{2+}$ currents evoked by a 5 ms, 20 mV step (S), followed by a series of 20 mV ramps, while the lower traces are the AII EPSCs. The RBC pipette contained the $Cs^{+}$-based internal solution. The duration of each ramp (in ms) is indicated above the voltage protocol. *B*, summary of the dependence of the EPSC peak (left) and area (right) on ramp duration ($n = 6$). Peak response for each ramp was normalized to the step response. For each cell, charge transfer was normalized to the largest value for that cell. Open symbol (right) indicates the charge transfer elicited by a 5 ms voltage step. *C*, left, $Ca^{2+}$ tail current elicited after a 5 ms ramp (which by itself did not produce an EPSC) produces a fast, transient EPSC. Right, tail current elicited after a 20 ms ramp (which did produce an EPSC) fails to evoke any additional release, although this stimulus was not sufficient to deplete the vesicle pool. Records are averages from 5 RBC–AII pairs. Bipolar cell pipette contained the $Cs^{+}$-based internal solution. Traces are a composite taken from 5 cell pairs. Only the end of each ramp is pictured (i.e. the repolarization from −37 to −57 mV).

RBC of the same speed, but different amplitudes, do not alter the size or shape of the AII EPSC (Fig. 3*B*).

### cGMP and the kinetics of transduction channel opening in RBCs

Our results suggest that the speed of RBC depolarization plays an important role in shaping the postsynaptic AII response. We tested this idea further using a different approach. During a light response, rod bipolar cells are depolarized by the opening of non-selective cation channels. We mimicked the postsynaptic effect of the light response by bathing the retina in the mGluR6 agonist L-AP4 (4 $\mu$M) and then applying brief puffs of the antagonist CPPG (600 $\mu$M) locally to the RBC dendrites. CPPG terminates G-protein signalling by binding to the mGluR6 receptor, resulting in the opening of cation-selective transduction channels and depolarization of the RBC. We have shown previously that cGMP acts on the mouse mGluR6 cascade to amplify postsynaptic responses to puffs of CPPG (Snellman & Nawy, 2004). Those experiments were performed under voltage clamp, and so here we first tested whether cGMP similarly potentiated current-clamped responses. This was accomplished using two different methods. In some experiments, cGMP was introduced into RBCs through the patch pipette. The dose–response plot for seven cells dialysed internally with cGMP is shown in Fig. 4*A*. As expected, cGMP potentiated responses to CPPG puffs in current clamp (Fig. 4*A*). The inset traces are an ensemble average from seven cells showing the response to three different puff lengths. The briefest puff of 5 ms failed to elicit a response in 4 of 7 cells within the first 2 min of break-in, and so the ensemble response is quite small (left). Also shown are the responses to puffs of 15 and 45 ms. After 10 min of recording, allowing for diffusion of cGMP into the dendrites, a 5 ms puff produced a response in all seven cells, and the response to longer puffs was also substantially potentiated (right). Similar results were obtained with bath application of 8-pCPT-cGMP, a membrane-permeant form of cGMP (Fig. 4*B*). The left side shows responses to three different durations of CPPG puffs. After treatment with 8-pCPT-cGMP, even the briefest puff produced a maximal response. Responses to CPPG could be recorded in current clamp from RBCs for up to an hour with minimal run-down, and run-up was never observed in the absence of cGMP. Thus, the overall effect of cGMP was to reduce the concentration

of CPPG required to open transduction channels, as has been posited previously (Snellman & Nawy, 2004).

In addition to potentiating the size of the puff response, cGMP had two additional effects that are both consistent with modulation of the mGluR6 transduction pathway. First, it decreased the latency of the response, as is illustrated from composite voltage- and current-clamp traces comprising seven voltage-clamped, and seven current-clamped RBCs (Fig. 4*C*). On average, cGMP decreased the latency (expressed as the time to 10% of peak) from $67 \pm 3$ ms to $57 \pm 3$ ms in current-clamp (Fig. 4*D*; $n = 7$). This is unlikely to result from an effect of cGMP on voltage-gated channels, as a similar overall reduction was observed in voltage-clamp ($75 \pm 5$ ms to $57 \pm 7$ ms; $n = 7$). The observed reduction in the overall latency is likely to be an underestimate of the effect of cGMP on the transduction latency, since the overall latency is composed of several fixed processes in addition to mGluR6 transduction, including the transit time of the puff solution to the RBC dendrites and the rate of unbinding of glutamate from the mGluR6 receptor. Second, cGMP also increased the rate of RBC depolarization (Fig. 4*D*). For example, the average rate of rise to a 45 ms puff of CPPG increased from $127 \pm 26$ mV s$^{-1}$ to $266 \pm 52$ mV s$^{-1}$ after exposure to cGMP ($n = 7$).

### Postsynaptic currents in AII amacrine cells evoked by CPPG puffs

Although modest compared with the fastest ramps, this increase in the rate, as well as the amplitude, of RBC depolarization might be expected to enhance the fast component of the AII EPSC. To test this prediction, we first voltage clamped AII amacrine cells and nearby RBCs. We determined whether the pairs were synaptically coupled by stepping the voltage in the RBC to elicit a response in the AII, before switching the RBC recording into current clamp mode. We then puffed CPPG onto the dendrites of the presynaptic RBC, simultaneously recording CPPG-evoked depolarization in the RBC and the subsequent EPSC evoked in the AII (Fig. 5*A*). Brief puffs of CPPG produced slow RBC depolarizations that typically elicited responses composed of a series of discrete events lasting for the duration of the CPPG application (upper panel). Higher concentrations of CPPG produced a faster and larger RBC depolarization, which decreased

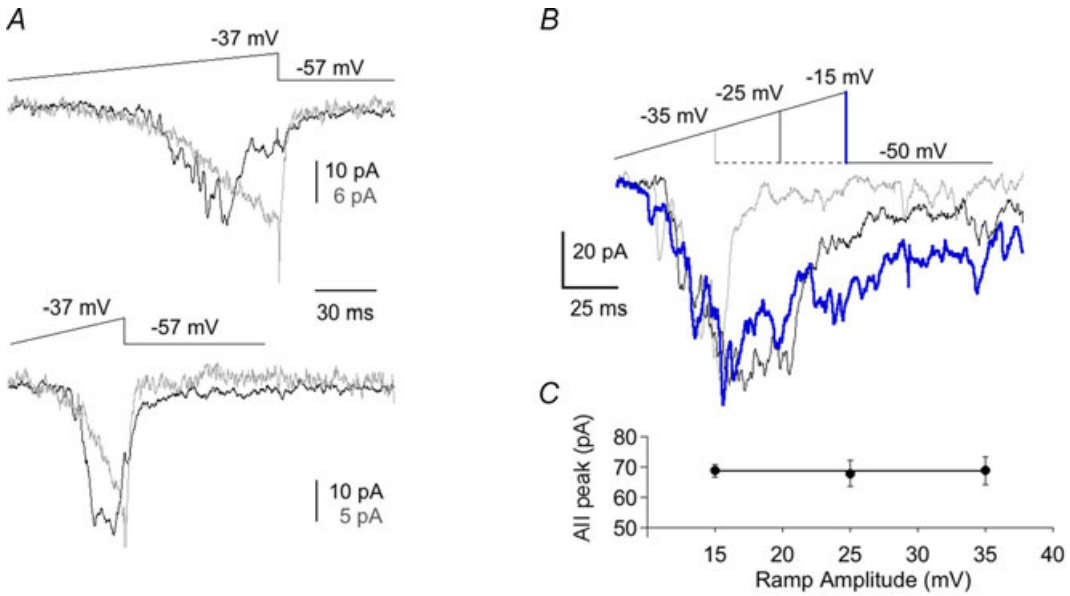


**Figure 3. The amplitude of the AII EPSC is not encoded by the magnitude of the presynaptic $I_{Ca}$**
*A*, responses of a **s**ynaptically coupled RBC and AII to a 140 ms 20 mV ramp (top), and a 60 ms 20 mV ramp (bottom). Note that for both stimulus durations, the peak of the AII response (black) leads the peak RBC calcium current (grey). This finding, which we observed in every RBC–AII pair that we recorded from, implies that the EPSC is encoded by the rate of rise of $I_{Ca}$ rather than the amplitude of the peak $I_{Ca}$. *B*, response of an AII to stimulation of a synaptically connected RBC with a series of ramps of increasing amplitude and duration (15, 25 and 35 mV lasting 50, 82 and 114 ms, respectively), but with the same rate of 0.3 mV ms$^{-1}$. Note the similarity in the peak amplitudes of the responses. *C*, summary of data collected from 3 AII amacrine cells in response to the stimulation protocol described in (*B*). The averaged peak responses are plotted as a function of ramp amplitude. Peak responses were not significantly different from each other for any stimulation condition.

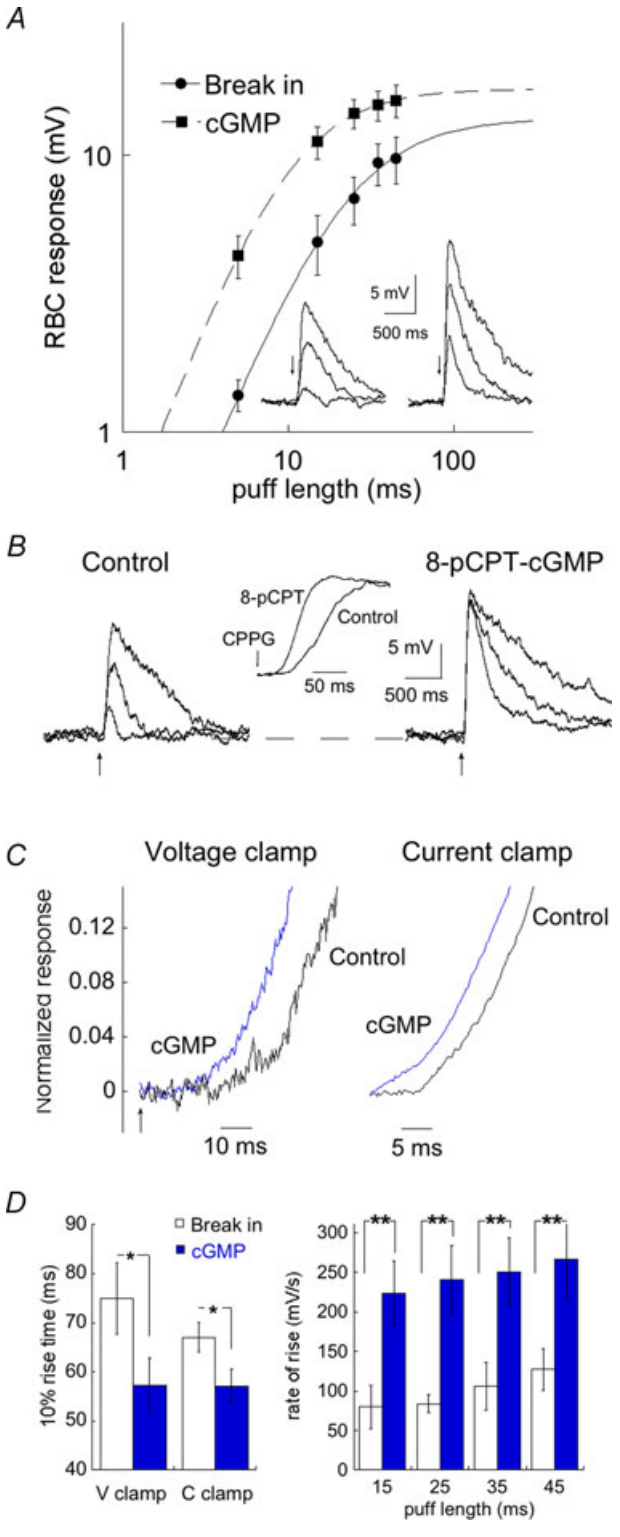


**Figure 4. cGMP modulates the amplitude and kinetics of current clamped responses to CPPG in RBCs**
*A*, summary of the relationship between CPPG (600 $\mu$M) puff length and RBC response at break-in and following diffusion of cGMP into the cell ($n = 7$). L-AP4 (4 $\mu$M) was present in the bath at all times. Inset, composite responses of 7 cells to CPPG puff durations of 5, 15 and 45 ms obtained immediately after break-in (left), and after 10 min of internal perfusion with 1 mM cGMP (right). Arrows indicate timing of the puff. *B*, responses to of 10, 50 and 200 ms puffs of CPPG in an RBC in control solution (left), and after a 10 min local application of 8-pCPT-cGMP. Inset, amplitude normalized responses to 200 ms puffs before and after application of 8-pCPT-cGMP shown on an expanded time base. Note the differences in latency and rate of rise. *C*, left, composite voltage clamp response from 7 RBCs recorded immediately after break-in and following dialysis with 1 mM cGMP. Cells were voltage-clamped at −62 mV. Puff duration was 200 ms. Right, composite response of 7 RBCs recorded in current clamp. Puff duration was 45 ms, and commenced 30 ms before the beginning of the trace. *D*, left, summary of the effect of cGMP (1 mM) on response latency, expressed as the time required for each response to reach 10% of the peak ($n = 7$). Puff durations as in *C*. Right, summary of effect of cGMP on the rate of rise of the current-clamped CPPG response as a function of puff length. The rate of rise for each response was calculated as the response amplitude/10–90% rise time ($n = 6$).

the latency of the EPSC. The EPSC evoked by stronger RBC depolarization was less discrete, as the higher frequency of release events fused to produce a sustained inward current. As with the response to briefer puffs of CPPG, the EPSC continued for the duration of RBC depolarization. The size of the AII EPSC was highly correlated with the rate of depolarization of the RBC, as is illustrated in Fig. 5*B*, which shows the relationship between EPSC peak and RBC rate of rise for four different puff lengths in five cell pairs. Presynaptic mGluRs have not been found on RBC terminals, and the presence of L-AP4 in the bath was found to have no effect on the kinetics or time course of the AII EPSC as compared to baseline (half-width $4.9 \pm 0.4$ *vs.* $4.8 \pm 0.3$, $n = 6$, $P < 0.7$).

Figure 5*C* compares the kinetics of the early phase of the EPSC in response to either a voltage step (upper panel) or the application of CPPG (lower panels). Note that the initial transient portion of the AII EPSC was significantly broader when it was evoked by CPPG compared with a voltage step. This is most likely to be due to a fundamental difference between the two protocols: the puff of CPPG most likely spread beyond the dendrites of the recorded RBC and depolarized neighbouring bipolar cells. The rising phase of each RBC would be smeared by differences in the time required for the CPPG puff to reach its targets. This might account for the observation that the transient component of the AII EPSC evoked by a puff of CPPG was always broader than when evoked by a voltage step.

### Potentiation of AII EPSCs by cGMP

We next examined the effect of modulation of the RBC response by cGMP on the amplitude and kinetics of the AII EPSC. Again, as with experiments on single RBCs, we either applied cGMP directly to single RBCs through the recording pipette, or we locally perfused membrane-permeant 8-pCPT-cGMP through a flowpipe (inset, Fig. 6*A*). The latter method has the advantage of insuring that responses in all RBCs stimulated by CPPG

were potentiated, and also allowed us to control the timing of cGMP delivery. As a control, we applied cGMP intracellularly to AII amacrine cells but saw no potentiation of the EPSC, indicating that the primary action of bath-applied cGMP is presynaptic ($n = 3$, data not shown). In addition, neither intracellular nor bath-applied cGMP had an effect on the kinetics of release from the RBC (half-width $4.8 \pm 0.4$, $n = 6$, $P < 0.6$ compared with baseline). Figure 6*A* illustrates the results of an experiment where 8-pCPT-cGMP was applied through a flowpipe. On the left is the response to a brief (8 ms) puff of CPPG before (black trace) and during perfusion of 8-pCPT-cGMP (blue trace in the online version). Both the amplitude and speed of the RBC response were dramatically increased by the cGMP analogue, and there was a concomitant increase in the amplitude of both the sustained and transient components of the AII EPSC. On the right is the response to a longer (200 ms) puff of CPPG. Prior to application of the cGMP analogue, the response amplitude in the RBC was nearly maximal, and the primary effect of cGMP was to decrease both the latency and the rise time of the RBC response. The faster rise of the RBC membrane potential strongly augmented the initial transient component of the AII EPSC, consistent with the idea that the amplitude of the transient component is predominantly a function of the rate of rise of the RBC membrane potential. This is illustrated in Fig. 6*B*, which plots the correlation between the rate of depolarization of the RBC and the amplitude of the initial phase of the EPSC for the pair depicted in Fig. 6*A*. Each point represents the response to one of three puff durations obtained before and during application

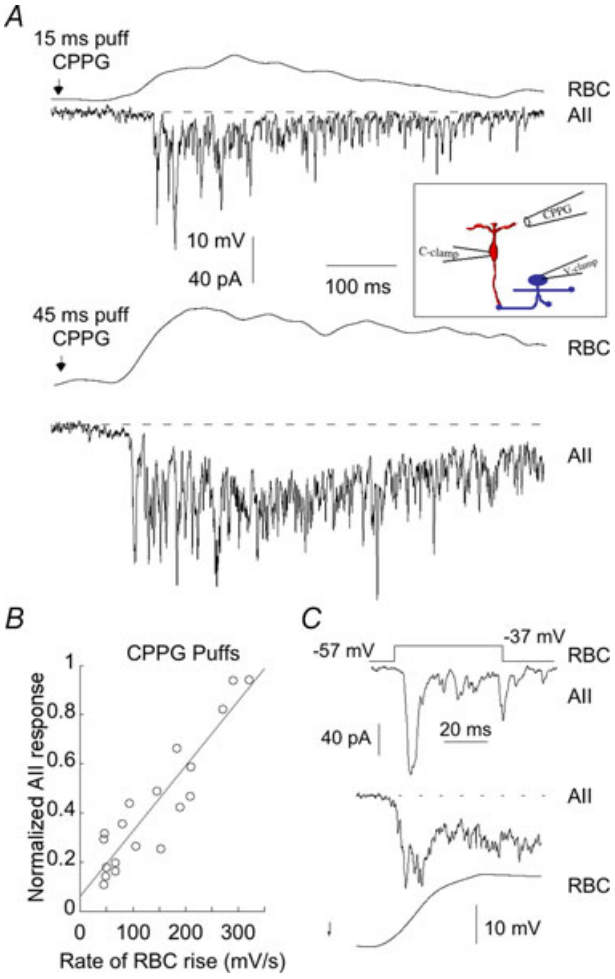


**Figure 5. Responses to puffs of CPPG resemble responses to slow ramps**
*A*, paired RBC and AII cells were current- and voltage-clamped respectively, and CPPG was puffed onto the dendrites of the RBC (inset). Response of an RBC–AII pair to a CPPG puff of 15 ms (top) and 45 ms (bottom). *B*, plot of the relationship between AII response and rate of rise of the associated RBC. Responses are to 4 different puff lengths (15, 25, 35, 45 ms) from 5 different pairs. $r^2 = 0.84$. *C*, comparison of the shape of the fast transient component of the EPSC in response to a voltage step in the RBC (top), or to a 45 ms puff of CPPG (middle and bottom traces). Puff responses are an average of 4 trials.

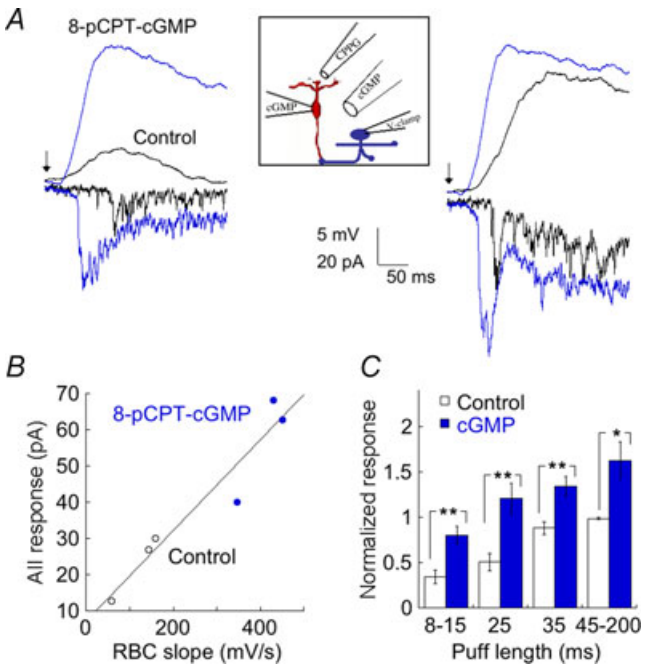


**Figure 6. Potentiation of RBC responses by cGMP in turn potentiates AII EPSCs**
*A*, averaged response of an RBC–AII pair to an 8 ms puff (left), or 50 ms puff (right) of CPPG following break in (black trace) and after local application of 1 mM 8-pCPT-cGMP (blue trace in the online version). Inset, experimental protocol; in some experiments, cGMP was dialysed directly into individual RBCs, while in others, such as the one shown here, it was added in a membrane-permeant form. *B*, left, effects of cGMP on the rate of depolarization of the RBC and the peak AII response from the pair shown in (*A*). Puff lengths were 8 ms, 35 ms and 200 ms. Open symbols are before and filled symbols are after 8-pCPT-cGMP application, respectively. *C*, summary of the effects of cGMP on AII response amplitude as a function of puff duration. Data from bath and intracellular application of cGMP have been pooled, and puff lengths have been binned as labelled. $n = 8$ for all puff length bins except for 25 ms ($n = 6$).

of 8-pCPT-cGMP. A good fit could also be obtained by plotting the size of the RBC response (data not shown); however the peak of the AII EPSC typically occurred well before the peak of the RBC response, suggesting that it is the rate of the RBC depolarization that is critical for encoding the amplitude of the EPSC. The effect of cGMP on AII EPSC amplitude is summarized for eight AII–RBC pairs in Fig. 6*C*.

Our data suggest that for weak RBC depolarizations, cGMP can potentiate both transient and sustained components of the EPSC by increasing the amount of depolarization. On the other hand, for strong depolarizations, cGMP potentiates primarily the transient component of the EPSC by speeding the kinetics of depolarization. Figure 7*A* illustrates the response of an AII amacrine cell to a strong stimulus (200 ms puff of CPPG) both before (left) and after (right) bath application of 8-pCPT-cGMP. Note that the cGMP analogue increased the transient component, but had little effect on the sustained component of the EPSC. To examine in more detail how cGMP altered the shape of the EPSC in response to strong presynaptic stimulation, we measured total charge transfer during the first 200 ms of the response, binned into 10 ms increments. We analysed four AII–RBC pairs, focusing on pairs where the longest puff durations represented the maximum depolarization of the RBC. For two AII amacrine cells, we analysed the response to the two longest puffs, both of which yielded nearly maximal EPSCs, while for the other two cells, we analysed only the longest puff. Each bin was then normalized to the total charge transfer during the first 200 ms of the EPSC, and thus the plot is a description of the contribution of the charge transfer at each time point to the total charge transfer. Following exposure to 8-pCPT-cGMP, the relative contribution of the early component of the response increased dramatically. For example, before 8-pCPT-cGMP application, the 50–60 ms bin contributed 2.4% of the total charge transfer, compared with 10.3% in its presence (Fig. 7*B*).

To determine the impact of cGMP on transmitter release, we calculated the number of vesicles released during the first 50 ms of the EPSC evoked by CPPG depolarization of the RBC. Before application of 8-pCPT-cGMP, we obtained a mean value of $9.4 \pm 1.3$ vesicles (Fig. 7*C*, $n = 6$). Application of the cGMP analogue increased the release to $25.5 \pm 4.4$ vesicles, a significant difference compared with control ($P < .01$), but it did not significantly change the amplitude of the RBC response to CPPG (control: $17.8 \pm 1.2$ mV, 8-pCPT-cGMP: $18.0 \pm 1.7$ mV, $P > 0.9$). Thus, even for strong stimuli that mimic saturating light conditions, cGMP can selectively enhance the transient component of the AII EPSC without markedly changing the steady state component by increasing the rate of RBC depolarization.

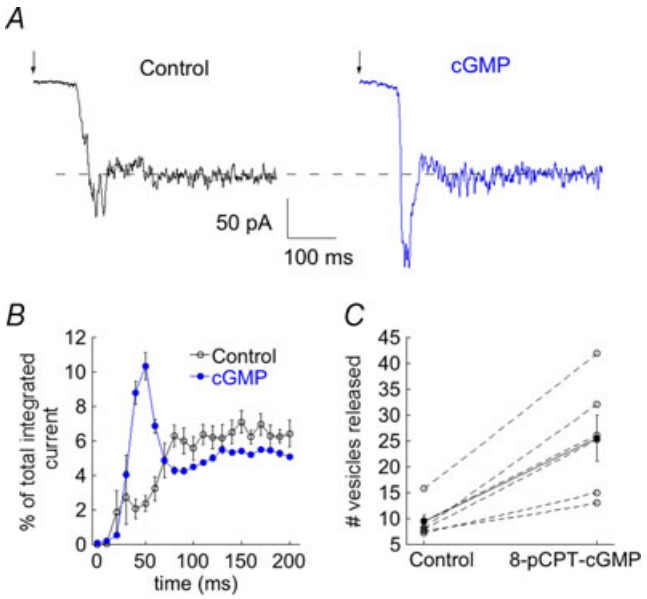


**Figure 7. cGMP accentuates specifically the fast component of the AII EPSC**
*A*, responses of an AII amacrine cell to a 50 ms puff of CPPG onto the outer plexiform layer (OPL) before (black) and during (blue in the online version) local application of 1 mM 8-pCPT-cGMP. Records are averages of 7 (control) and 3 (cGMP) trials from the same cell. *B*, analysis of the first 200 ms of the EPSC in response to saturating puffs of CPPG for 4 amacrine cells before (open symbols) and after (filled symbols) 8-pCPT-cGMP application. Each point, representing charge transfer during a 10 ms window, has been normalized to the total charge transfer measured during the 200 ms period. Overall, 8-pCPT-cGMP shifted the distribution of charge transfer toward the first 50 ms of the EPSC. *C*, summary of the effect of 8-pCPT-cGMP on the number of vesicles released during the first 50 ms of the EPSC. Data are from 2 puff lengths in 2 cells and 1 puff lengths in 2 other cells. Filled symbols indicate mean/S.E.M.

## Discussion

When using voltage steps to stimulate release from RBC terminals, we observe a large, transient component of the AII amacrine cell EPSC, followed by a small sustained component. The kinetics of this response have been reported in detail elsewhere (Singer & Diamond, 2003, 2006; Singer *et al.* 2004; Trexler *et al.* 2005). The fast, transient component has been attributed to a rapid emptying of the RRP, followed by a very small sustained component, whose amplitude is thought to reflect the rate of vesicle replenishment (Singer & Diamond, 2006). However, light-evoked responses in the AII amacrine cells of cat, rabbit and mouse over a wide range of intensities, while somewhat transient, reveal a far greater balance between transient and steady-state components than do step-evoked responses (Nelson, 1982; Xin & Bloomfield, 1999; Bloomfield & Xin, 2000; Volgyi *et al.* 2002; Wu *et al.* 2004; Trexler *et al.* 2005; Dunn *et al.*

2006; Pang *et al.* 2007). This discrepancy between light and voltage-step evoked responses in AII amacrine cells might be explained by differences in the magnitude of presynaptic signal, particularly for dim stimuli. However, at higher flash intensities, the magnitude of the RBC response can reach 25–30 mV (Berntson & Taylor, 2000; Euler & Masland, 2000; Trexler *et al.* 2005). Assuming a dark resting potential of −55 mV, the midpoint in the reported range of ON bipolar dark potentials (Awatramani & Slaughter, 2000; Euler & Masland, 2000; Ichinose *et al.* 2005), this magnitude of depolarization would be ideal for L-type $Ca^{2+}$ channel activation in the RBC terminal (Protti, 1998; Pan, 2000). Yet at these flash intensities, the sustained component of the EPSC, relative to the transient component, is nearly an order of magnitude larger compared with responses to voltage steps (Trexler *et al.* 2005). Likewise, in the present study, we find that puffs of CPPG which evoked 20 mV responses in RBCs elicited smaller, more sustained AII EPSCs than did voltage steps of the same magnitude.

Instead, our study suggests that it is the speed of depolarization, rather than simply the amplitude, that is critical for evoking a large transient component. Direct evidence for this comes from experiments where we varied the rate of RBC depolarization with a series of ramps of constant amplitude (20 mV) but different velocities (range: 200–2000 mV $s^{-1}$). This protocol reveals an inverse correlation between the speed of RBC depolarization and the size of the transient component of the EPSC. Slow ramps elicited no clear peak at all, but rather a series of discrete events, presumably corresponding to individual release events. Interestingly, the slower ramps correspond to the rate of rise of RBC light responses in mouse retina, around 400 mV $s^{-1}$ (from Fig. 3 of Berntson & Taylor, 2000) (see also Euler & Masland, 2000). Thus, under physiological conditions, the RBC–AII synapse may normally function at the slow end of the range of ramp speeds that we examined.

What mechanisms might account for the filtering of slow depolarizations? It cannot be accounted for by a lack of $Ca^{2+}$ influx, as even the slowest ramps that we tested activated $Ca^{2+}$ current, and there was no significant difference between current amplitudes evoked by slow and fast ramps. More likely, the ramp experiments reveal a more general mechanism for limiting vesicle release over time. Experiments described in Fig. 1 provide evidence for a limited time window during which rapid release of vesicles can be achieved. For very large depolarizations, depletion of the RRP of vesicles might account for this limited time period of release (Singer & Diamond, 2003, 2006). However, we find that this time window is present even under conditions where it is unlikely that the RRP has been depleted. Thus it seems that other mechanisms, in addition to vesicle depletion, contribute to the time course of release of the RRP from RBC terminals.

In goldfish bipolar cell terminals, it has been suggested that a second mechanism underlying depression of release, in addition to depletion, might be a differential sensitivity to $Ca^{2+}$; vesicles furthest from sites of $Ca^{2+}$ entry would be released more slowly, or perhaps not at all if endogenous buffers are sufficient to keep pace with the influx of $Ca^{2+}$ (Burrone & Lagnado, 2000; Burrone *et al.* 2002). Rapid influx of $Ca^{2+}$, as would occur during a voltage step or fast ramp, would saturate the buffering capacity of the mobile $Ca^{2+}$ buffer (EGTA in our experiments) before diffusion of unbound EGTA into the $Ca^{2+}$ domain had an opportunity to occur. Slower influx of $Ca^{2+}$, as during the ramps, might result in a functionally larger $Ca^{2+}$ buffering capacity (Burrone & Lagnado, 2000). Alternatively, the duration of the EPSC transient component might be limited by a $Ca^{2+}$ feedback mechanism in the RBC terminal (Hsu *et al.* 1996). This mechanism could set a fixed time window for release from the RRP. Beyond this time, release might come from a separate pool, or perhaps from the RRP, but at a much lower rate, accounting for the maintained phase of the EPSC. In this model, rapid depolarization of the RBC terminal allows for greater $Ca^{2+}$ influx and hence more release during the critical time window. Slower depolarizations position the time of greatest $Ca^{2+}$ influx beyond this window, thus attenuating the initial phase of transmitter release. The ability of the synapse to switch from a fast to a slow mode of release would prevent vesicle depletion during maintained periods of illumination, while still allowing for the detection and transmission of rapid changes in light intensity.

A second goal of this study was to extend our previous findings on the modulation of mGluR6 signal transduction by cGMP (Snellman & Nawy, 2004). Here, as was reported previously, we find that small responses to brief puffs of CPPG are strongly potentiated in the presence of cGMP. Because of the threshold imposed by the RBC–AII synapse, responses evoked by CPPG that were smaller than about 5 mV generally did not evoke detectable EPSCs. Thus we envision that cGMP, by increasing the amplitude of small events, would enable a higher proportion of events to exceed the minimal threshold for transmission in the inner retina. Rod bipolar cells have the machinery necessary to produce endogenous cGMP, as they express soluble guanylate cyclase (Ding & Weinberg, 2007). Furthermore, the endogenous level of cGMP and the synaptic response in rod bipolar cells are potentiated by activation of guanylate cyclase with nitric oxide donors (Cao *et al.* 2000; Snellman & Nawy, 2004; Pong & Eldred, 2009). Inhibition of cGMP-dependent protein kinase (cGK) attenuates synaptic responses in rod bipolar cells (Snellman & Nawy, 2004), suggesting that the endogenous level of cGMP is sufficient to activate cGK. While advantageous for increasing absolute sensitivity, amplification might also contribute to noise postulated to

be generated at the RBC–AII amacrine cell synapse (Dunn *et al.* 2006).

At longer puff durations, the effect of cGMP on RBC amplitude was less pronounced. Here, the primary effect of cGMP was to speed the rate of rise and shorten the latency of the RBC response. As discussed above, a speeding of the rising phase resulted in a potentiation of the peak AII EPSC. It has been suggested that the activated mGluR6–$G_{\alpha}o$ complex may generate a substance that binds to and closes the synaptic channel. When the mGluR6 receptors are fully bound by agonist, the levels of channel-closing compound are in excess of what is needed to hold the synaptic channels closed (Shiells & Falk, 1994; van Rossum & Smith, 1998; Field & Rieke, 2002). During the puff response, when the G-protein complex is shut off, this excess pool of channel-closing substance would need to be depleted before the synaptic channels could begin opening. The time required for pool depletion would contribute to the latency of channel opening following administration of the puff. Both the decrease in latency and the increased rate of rise are consistent with the idea that cGMP increases the rate of degradation of this substance following shut off of the mGluR6–$G_{\alpha}\bar{o}$ complex: an increased degradation rate would shorten the lifetime of the excess pool of channel-closing substance, leading to a decrease in latency. It would also result in an increased opening rate of the synaptic channels and consequently faster depolarization. The shortened latency and accelerated rising phase of the RBC response would also contribute to the characteristic speeding of the rod response that is a hallmark of the AII amacrine cell (Nelson, 1982).

## References


Awatramani GB & Slaughter MM (2000). Origin of transient and sustained responses in ganglion cells of the retina. *J Neurosci* **20**, 7087–7095.

Berntson A, Smith RG & Taylor WR (2004). Transmission of single photon signals through a binary synapse in the mammalian retina. *Vis Neurosci* **21**, 693–702.

Berntson A & Taylor WR (2000). Response characteristics and receptive field widths of on-bipolar cells in the mouse retina. *J Physiol* **524**, 879–889.

Bloomfield SA (2001). Plasticity of AII amacrine cell circuitry in the mammalian retina. *Prog Brain Res* **131**, 185–200.

Bloomfield SA & Xin D (2000). Surround inhibition of mammalian AII amacrine cells is generated in the proximal retina. *J Physiol* **523**, 771–783.

Burrone J & Lagnado L (2000). Synaptic depression and the kinetics of exocytosis in retinal bipolar cells. *J Neurosci* **20**, 568–578.

Burrone J, Neves G, Gomis A, Cooke A & Lagnado L (2002). Endogenous calcium buffers regulate fast exocytosis in the synaptic terminal of retinal bipolar cells. *Neuron* **33**, 101–112.

Cao L, Blute TA & Eldred WD (2000). Localization of heme oxygenase-2 and modulation of cGMP levels by carbon monoxide and/or nitric oxide in the retina. *Visual Neurosci* **17**, 319–329.

Chavez AE & Diamond JS (2008). Diverse mechanisms underlie glycinergic feedback transmission onto rod bipolar cells in rat retina. *J Neurosci* **28**, 7919–7928.

Chavez AE, Singer JH & Diamond JS (2006). Fast neurotransmitter release triggered by Ca influx through AMPA-type glutamate receptors. *Nature* **443**, 705–708.

Ding JD & Weinberg RJ (2007). Distribution of soluble guanylyl cyclase in rat retina. *J Comp Neurol* **500**, 734–745.

Dunn FA, Doan T, Sampath AP & Rieke F (2006). Controlling the gain of rod-mediated signals in the mammalian retina. *J Neurosci* **26**, 3959–3970.

Eggers ED & Lukasiewicz PD (2006). Receptor and transmitter release properties set the time course of retinal inhibition. *J Neurosci* **26**, 9413–9425.

Euler T & Masland RH (2000). Light-evoked responses of bipolar cells in a mammalian retina. *J Neurophysiol* **83**, 1817–1829.

Field GD & Rieke F (2002). Nonlinear signal transfer from mouse rods to bipolar cells and implications for visual sensitivity. *Neuron* **34**, 773–785.

Hartveit E (1999). Reciprocal synaptic interactions between rod bipolar cells and amacrine cells in the rat retina. *J Neurophysiol* **81**, 2923–2936.

Hsu S-F, Augustine GJ & Jackson MB (1996). Adaptation of $Ca^{2+}$-triggered exocytosis in presynaptic terminals. *Neuron* **17**, 501–512.

Ichinose T, Shields CR & Lukasiewicz PD (2005). Sodium channels in transient retinal bipolar cells enhance visual responses in ganglion cells. *J Neurosci* **25**, 1856–1865.

Mennerick S & Matthews G (1996). Ultrafast exocytosis elicited by calcium current in synaptic terminals of retinal bipolar neurons. *Neuron* **17**, 1241–1249.

Nakajima Y, Iwakabe H, Akazawa C, Nawa H, Shigemoto R, Mizuno N & Nakanishi S (1993). Molecular characterization of a novel retinal metabotropic glutamate receptor mGluR6 with a high agonist selectivity for L-2-amino-4-phosphonobutyrate. *J Biol Chem* **268**, 11868–11873.

Nawy S (2004). Desensitization of the mGluR6 transduction current in tiger salamander On bipolar cells. *J Physiol* **558**, 137–146.

Nelson R (1982). AII amacrine cells quicken time course of rod signals in the cat retina. *J Neurophysiol* **47**, 928–947.

Palmer MJ, Hull C, Vigh J & von Gersdorff H (2003). Synaptic cleft acidification and modulation of short-term depression by exocytosed protons in retinal bipolar cells. *J Neurosci* **23**, 11332–11341.

Pan Z-H (2000). Differential expression of high- and two types of low-voltage-activated calcium currents in rod and cone bipolar cells of the rat retina. *J Neurophysiol* **83**, 513–527.

Pang J-J, Abd-El-Barr MM, Gao F, Bramblett DE, Paul DL & Wu SM (2007). Relative contributions of rod and cone bipolar cell inputs to AII amacrine cell light responses in the mouse retina. *J Physiol* **580**, 397–410.

Pong WW & Eldred WD (2009). Interactions of the gaseous neuromodulators nitric oxide, carbon monoxide, and hydrogen sulfide in the salamander retina. *J Neurosci Res* (in press).

Protti DA & Llano I (1998). Calcium current and calcium signaling in rod bipolar cells of rat retina slices. *J Neurosci* **18**, 3715–3724.

Protti DA, Flores-Herr N & von Gersdorff H (2000). Light evokes $Ca^{2+}$ spikes in the axon terminal of a retinal bipolar cell. *Neuron* **25**, 215–227.

Robson JG & Frishman LJ (1995). Response linearity and kinetics of the cat retina: the bipolar cell component of the dark-adapted electroretinogram. *Vis Neurosci* **12**, 837–850.

Saszik SM, Robson JG & Frishman LJ (2002). The scotopic threshold response of the dark-adapted electroretinogram of the mouse. *J Physiol* **543**, 899–916.

Shiells RA & Falk G (1994). Responses of rod bipolar cells isolated from dogfish retinal slices to concentration-jumps of glutamate. *Vis Neurosci* **11**, 1175–1183.

Shiells RA, Falk G & Naghshineh S (1981). Action of glutamate and aspartate analogues on rod horizontal and bipolar cells. *Nature* **294**, 592–594.

Singer JH & Diamond JS (2003). Sustained $Ca^{2+}$ entry elicits transient postsynaptic currents at a retinal ribbon synapse. *J Neurosci* **23**, 10923–10933.

Singer JH & Diamond JS (2006). Vesicle depletion and synaptic depression at a mammalian ribbon synapse. *J Neurophysiol* **95**, 3191–3198.

Singer JH, Lassova L, Vardi N & Diamond JS (2004). Coordinated multivesicular release at a mammalian ribbon synapse. *Nat Neurosci* **7**, 826–833.

Slaughter MM & Miller RF (1981). 2-Amino-4-phosphonobutyric acid: a new pharmacological tool for retina research. *Science* **211**, 182–185.

Snellman J & Nawy S (2002). Regulation of the retinal bipolar cell mGluR6 pathway by calcineurin. *J Neurophysiol* **88**, 1088–1096.

Snellman J & Nawy S (2004). cGMP-dependent kinase regulates response sensitivity of the mouse On bipolar cell. *J Neurosci* **24**, 6621–6628.

Trexler EB, Li W & Massey SC (2005). Simultaneous contribution of two rod pathways to AII amacrine and cone bipolar cell light responses. *J Neurophysiol* **93**, 1476–1485.

van Rossum MC & Smith RG (1998). Noise removal at the rod synapse of mammalian retina. *Vis Neurosci* **15**, 809–821.

Vardi N, Morigiwa K, Wang TL, Shi YJ & Sterling P (1998). Neurochemistry of the mammalian cone 'synaptic complex'. *Vision Res* **38**, 1359–1369.

Veruki ML, Morkve SH & Hartveit E (2003). Functional properties of spontaneous EPSCs and non-NMDA receptors in rod amacrine (AII) cells in the rat retina. *J Physiol* **549**, 759–774.

Veruki ML, Morkve SH & Hartveit E (2006). Activation of a presynaptic glutamate transporter regulates synaptic transmission through electrical signaling. *Nat Neurosci* **9**, 1388–1396.

Volgyi B, Xin D & Bloomfield SA (2002). Feedback inhibition in the inner plexiform layer underlies the surround-mediated responses of AII amacrine cells in the mammalian retina. *J Physiol* **539**, 603–614.

von Gersdorff H, Sakaba T, Berglund K & Tachibana M (1998). Submillisecond kinetics of glutamate release from a sensory synapse. *Neuron* **21**, 1177–1188.

Wersinger E, Schwab Y, Sahel JA, Rendon A, Pow DV, Picaud S & Roux MJ (2006). The glutamate transporter EAAT5 works as a presynaptic receptor in mouse rod bipolar cells. *J Physiol* **577**, 221–234.

Wolfel M, Lou X & Schneggenburger R (2007). A mechanism intrinsic to the vesicle fusion machinery determines fast and slow transmitter release at a large CNS synapse. *J Neurosci* **27**, 3198–3210.

Wu SM, Gao F & Pang J-J (2004). Synaptic circuitry mediating light-evoked signals in dark-adapted mouse retina. *Vision Res* **44**, 3277–3288.

Xin D & Bloomfield SA (1999). Comparison of the responses of AII amacrine cells in the dark- and light-adapted rabbit retina. *Vis Neurosci* **16**, 653–665.

## Author contributions

S.N., J.S. and D.Z. conceived and designed the experiments; J.S. carried out the experiments; S.N. and J.S. performed data analysis; S.N. and J.S. co-wrote the paper. S.N, J.S. and D.Z. revised the paper. Experiments were carried out at in the laboratories of S.N. and D.Z.

## Acknowledgements

We thank Drs Diana Pettit and Reed Carroll for valuable discussions. This work was supported by funding from the National Eye Institute to D.Z. (EY014990) and S.N. (EY010254).